Controlling interactions between peptide-heme and G-quadruplex DNA using Fe-bound NH_3 and H_2O ligands

Jing Liu, Jinyang Feng, Ze Sun, Chang Xin, and Hulin Tai*

* taihulin@ybu.edu.cn

Table of Contents

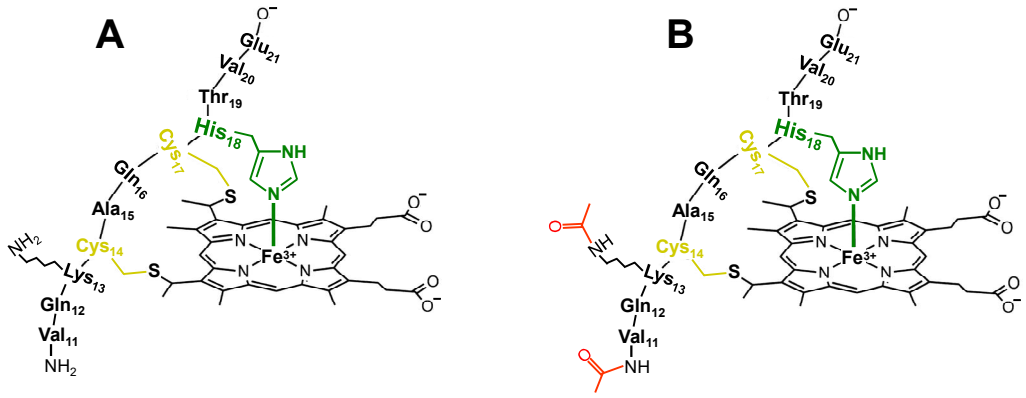

Figure S1 Molecular structures of the MP11 (A) and AcMP11 (B).

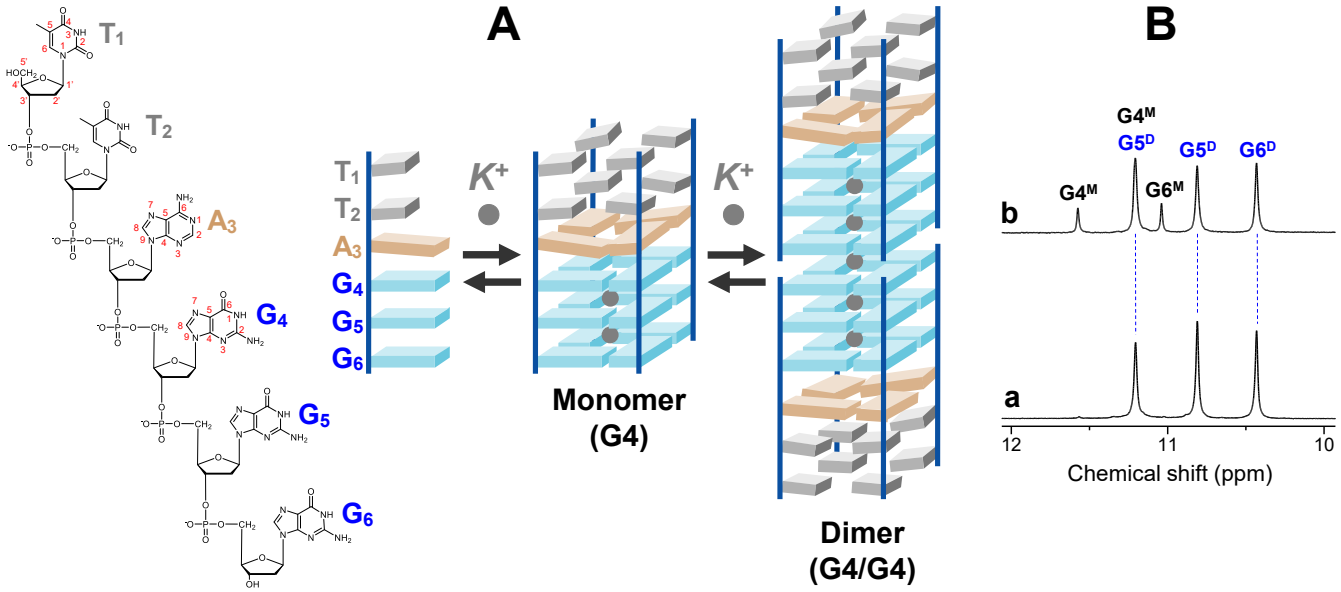

Figure S2 (A) Schematic representation of a parallel G-quadruplex DNA ([d(TTAGGG)]$_4$) formed from d(TTAGGG). (B) Downfield-shifted portions of the ^{1}H NMR spectra of the [d(TTAGGG)]$_4$ in 90% H_2O/10% D_2O, 50 mM potassium phosphate buffer (pH 7.00, 25°C), with (a) and without (b) 300 mM KCl.

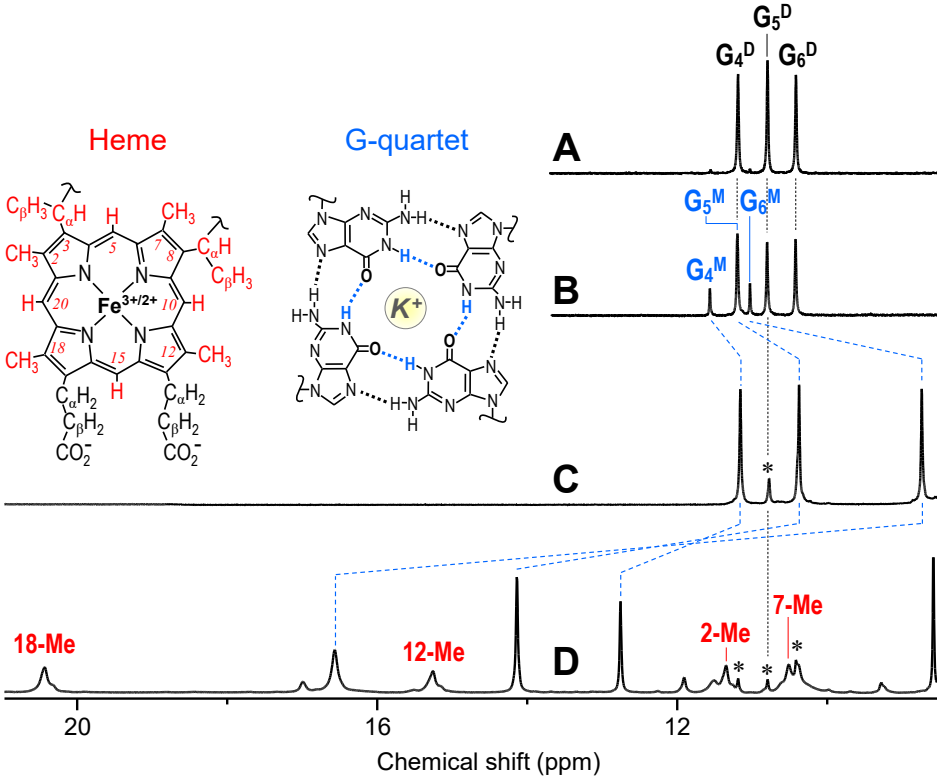

Figure S3 Down-shifted portions of the ^{1}H NMR spectra of [d(TTAGGG)]$_4$ (A and B), reduced Peptide-Heme(Fe^{2+})-NH_3/G4 hybrid complex (C), and oxidized Peptide-Heme(Fe^{3+})-NH_3/G4 hybrid complex (D) in 90% H_2O/10% D_2O, 50 mM potassium phosphate buffer (pH 7.0 and 25 °C), and with (A, C, D) and without (B) of 300 mM KCl. The reduced and oxidized Peptide-Heme($Fe^{2+/3+}$)-NH_3/G4 hybrid complex (C and D) were prepared in 150 mM NH_4Cl with and without of 150 equivalents $Na_2S_2O_4$. G_n^D and G_n^M, where n = 4, 5, 6, represent the dimer and monomer of the DNA. The molecular structures of *c*-type heme and G-quartet are shown in the upper left corner. The guanine imino proton signals of the free DNA and complexes are connected by broken lines. Peaks denoted asterisks in spectra C and D are due to the dimer DNA remaining in the samples.

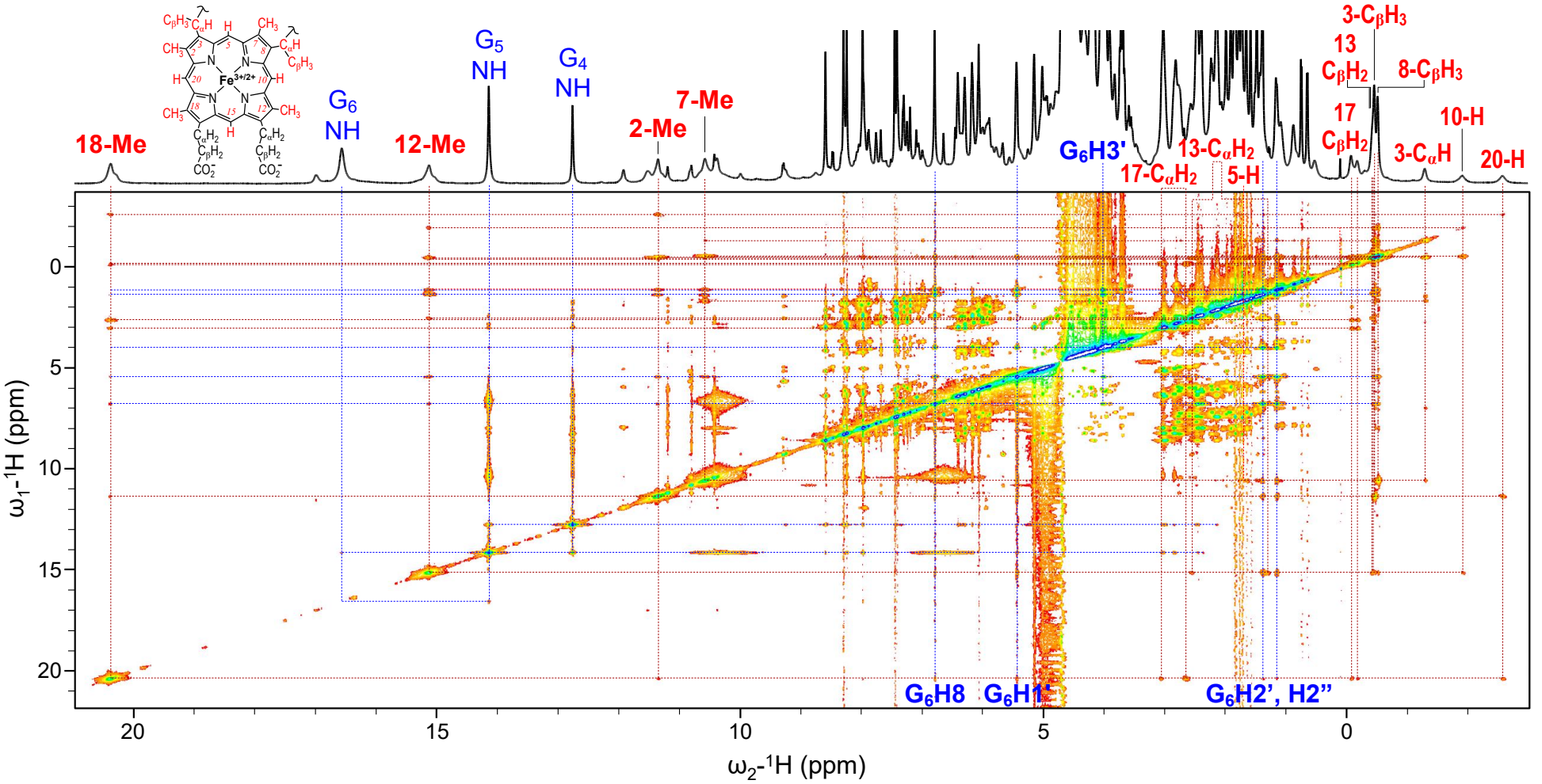

Figure S4 NOESY spectrum of the oxidized Peptide-Heme(Fe^{3+})-NH_3/G4 hybrid complex in 90% H_2O/10% D_2O, 150 mM NH_4Cl, 300 mM KCl, and 50 mM potassium phosphate buffer (pH 7.00, 25°C). A mixing time of 200 ms was used to record the spectrum. Assignments of heme side chain proton signals are shown. Assignments of DNA base proton signals are shown in Figures S5-S8.

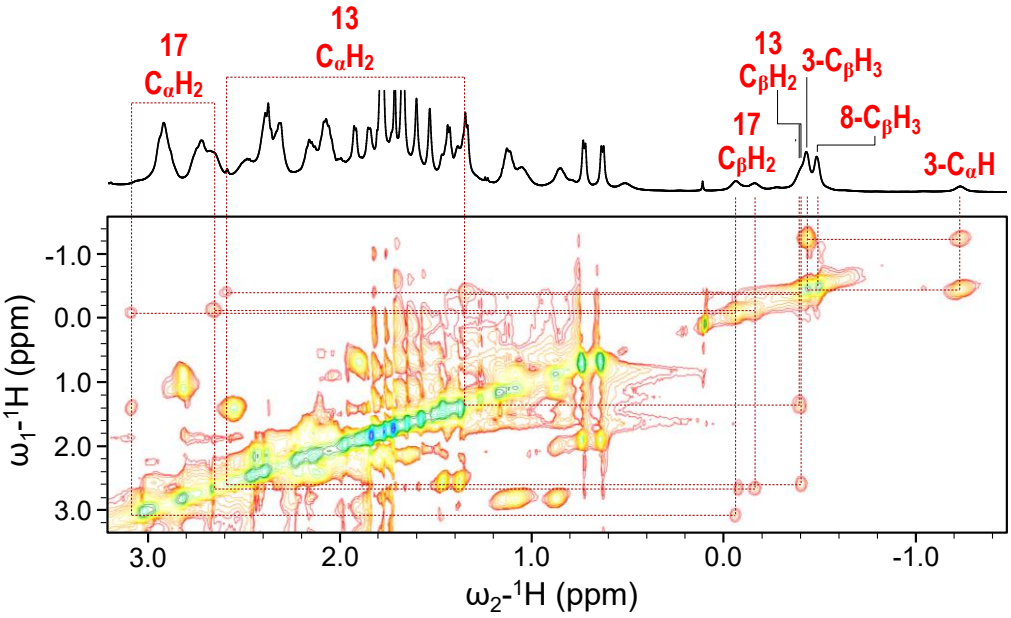

Figure S5 Portion of the TOCSY spectrum of the oxidized Peptide-Heme(Fe^{3+})-NH_3/G4 hybrid complex in 90% H_2O/10% D_2O, 150 mM NH_4Cl, 300 mM KCl, and 50 mM potassium phosphate buffer (pH 7.00, 25°C). A mixing time of 80 ms was used to record the spectrum. Assignments of selected proton signals are shown.

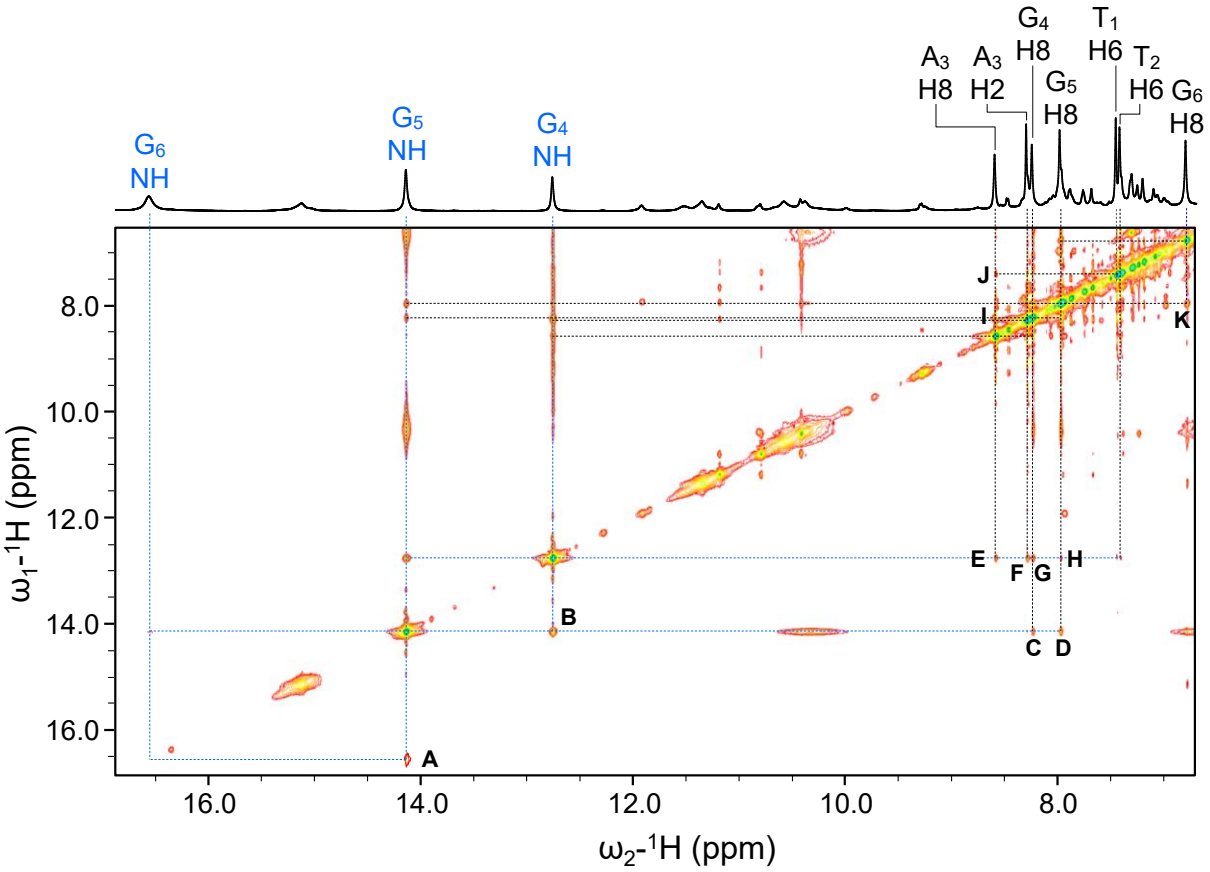

Figure S6 Portion of the NOESY spectrum of the oxidized Peptide-Heme(Fe^{3+})-NH_3/G4 hybrid complex in 90% H_2O/10% D_2O, 150 mM NH_4Cl, 300 mM KCl, and 50 mM potassium phosphate buffer (pH 7.00, 25°C). A mixing time of 200 ms was used to record the spectrum. Cross peaks A–K indicate the NOE connectivities of the following proton pairs: (A) G_6NH-G_5NH; (B) G_5NH-G_4NH; (C) G_5NH-G_4H8; (D) G_5NH-G_5H8; (E) G_4NH-A_3H8; (F) G_4NH-A_3H2; (G) G_4NH-G_4H8; (H) G_4NH-G_5H8; (I) A_3H8-G_4H8; (J) A_3H8-T_2H6; (K) G_5H8-G_6H8. Assignments of DNA base proton signals are shown.

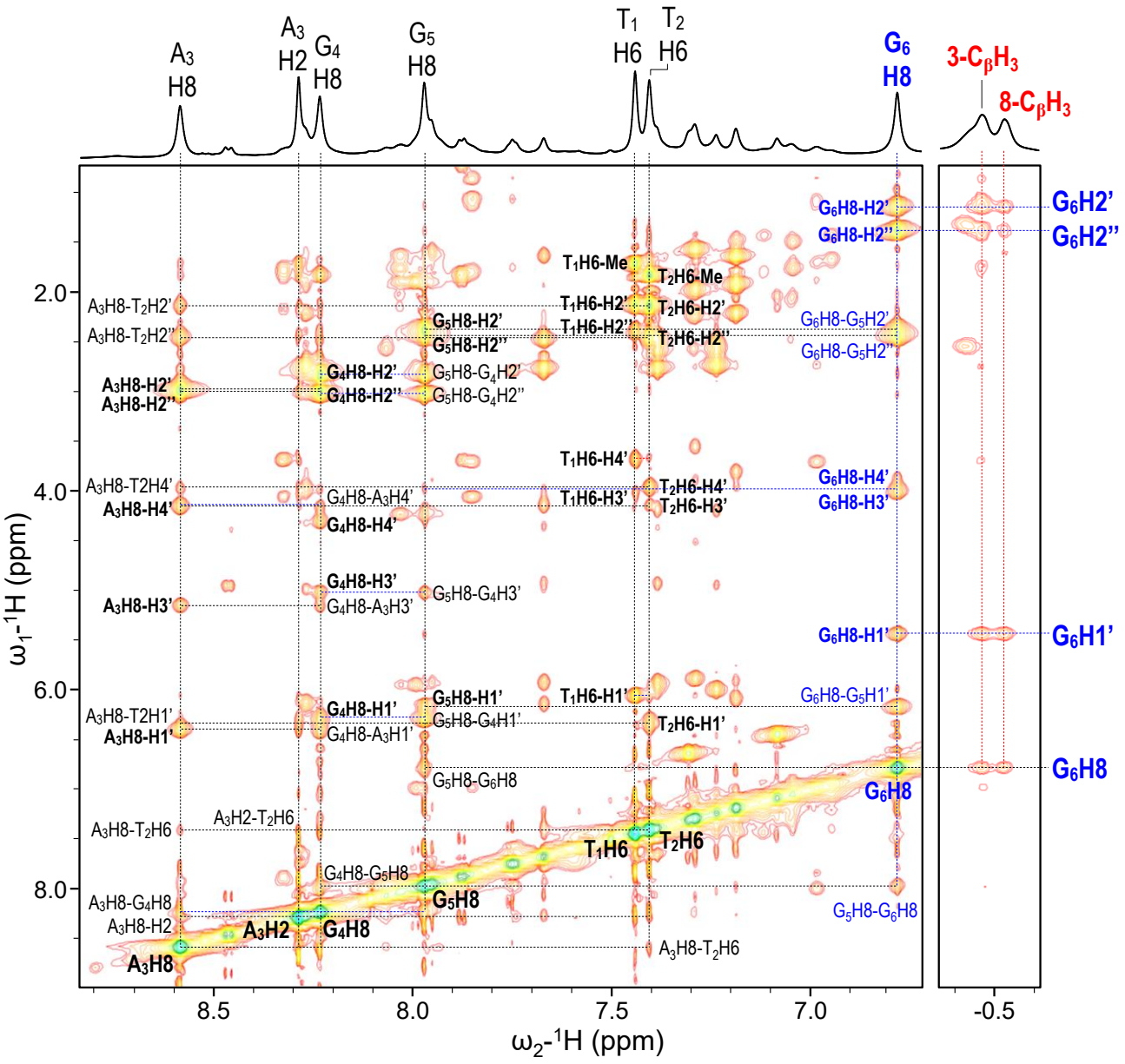

Figure S7 Portions of the NOESY spectrum of the oxidized Peptide-Heme(Fe^{3+})-NH_3/G4 hybrid complex in 90% H_2O/10% D_2O, 150 mM NH_4Cl, 300 mM KCl, and 50 mM potassium phosphate buffer (pH 7.00, 25°C). A mixing time of 200 ms was used to record the spectrum. Intramolecular NOE connectivities between base and ribose proton signals are shown in the left portion. Intermolecular NOE connectivities between heme side chain (3-$C_\beta H_3$ and 8-$C_\beta H_3$) and G_6-quartet (H8, H1', H2', and H2'') proton signals are shown in the right portion.

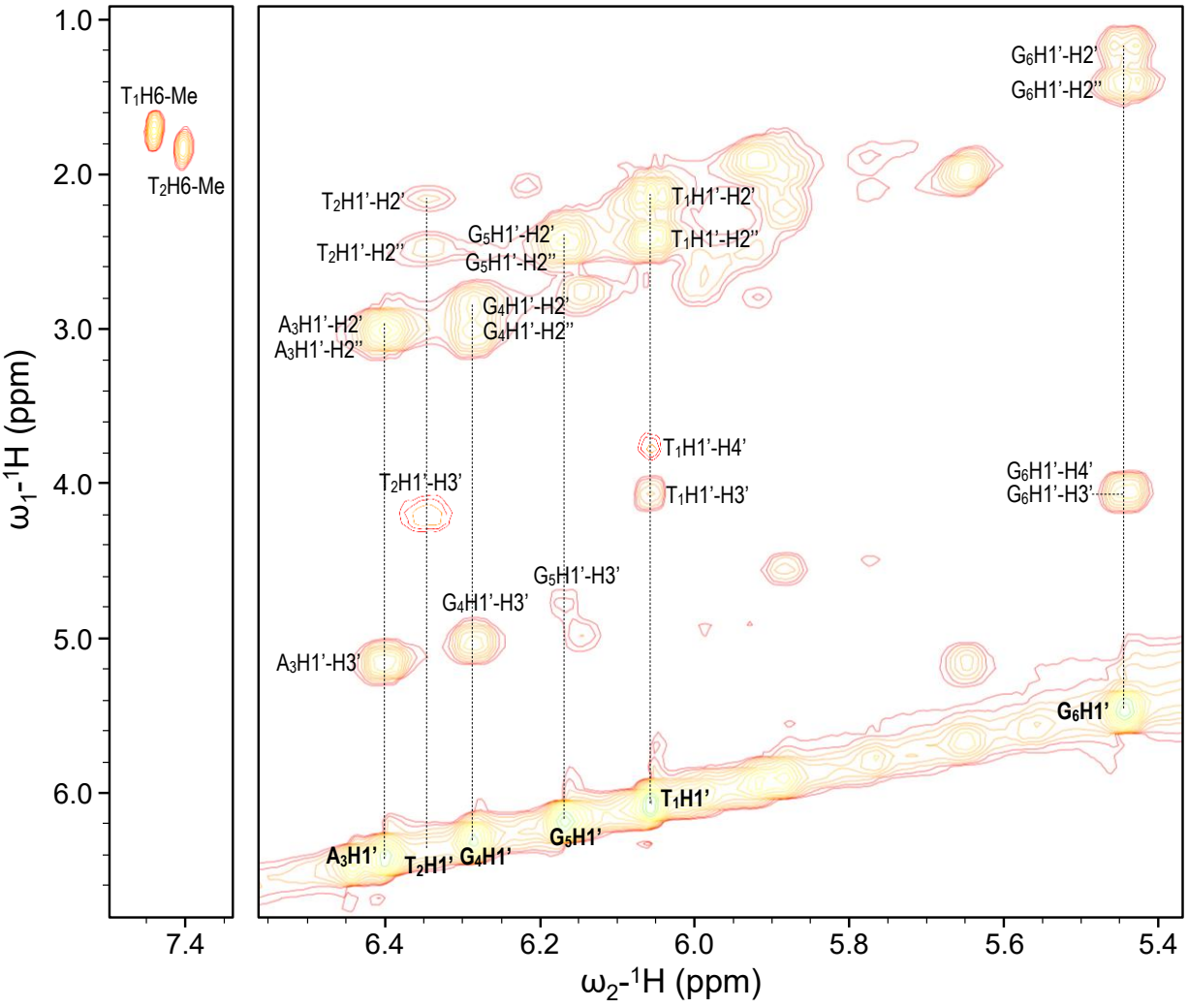

Figure S8 Portions of the TOCSY spectrum of the oxidized Peptide-Heme(Fe^{3+})-NH_3/G4 hybrid complex in 90% H_2O/10% D_2O, 150 mM NH_4Cl, 300 mM KCl, and 50 mM potassium phosphate buffer (pH 7.00, 25°C). A mixing time of 80 ms was used to record the spectrum. Assignments of selected base (thymine (T_1 and T_2), left portion) and ribose (right portion) proton signals are shown.

Table S1 Chemical shifts of the oxidized Peptide-Heme(Fe^{3+})-NH_3/G4 hybrid complex in 90% H_2O/10% D_2O, 150 mM NH_4Cl, 300 mM KCl, and 50 mM potassium phosphate buffer (pH 7.00, 25°C).

DNA	**Base protons**		**Ribose protons**			
	NH, Me,or H2	**H6 or H8**	**H1'**	**H2'/H2"**	**H3'**	**H4'**
T_1	1.72	7.44	6.06	2.13, 2.39	4.03	3.67
T_2	1.84	7.41	6.34	2.14, 2.45	4.14	3.97
A_3	8.29	8.59	6.40	2.97, 3.02	5.14	4.17
G_4	12.75	8.23	6.29	2.84, 3.01	5.01	4.31
G_5	14.14	7.97	6.17	2.39, 2.40	4.24	n.d.[a]
G_6	16.56	6.78	5.43	1.15, 1.38	4.03	3.99

Hemin	**Methyl protons**				**Thioether groups**				**Meso protons**			
	18-Me	**12-Me**	**7-Me**	**2-Me**	**3-C_αH**	**3-$C_\beta H_3$**	**8-C_αH**	**8-$C_\beta H_3$**	**5-H**	**10-H**	**15-H**	**20-H**
	20.37	15.12	10.58	11.34	-1.30	-0.47	n.d.[a]	-0.53	1.69	-1.92	n.d.[a]	-2.58

[a] Not determined.

Table S2 Chemical shifts of the reduced Peptide-Heme(Fe^{2+})-NH_3/G4 hybrid complex in 90% H_2O/10% D_2O, 150 mM NH_4Cl, 300 mM KCl, and 50 mM potassium phosphate buffer (pH 7.0, 25°C).

DNA	**Base protons**	
	NH, Me,or H2	**H6 or H8**
T_1	1.59	7.30
T_2	1.64	7.20
A_3	7.97	8.28
G_4	11.18	7.71
G_5	10.40	7.55
G_6	8.77	7.99

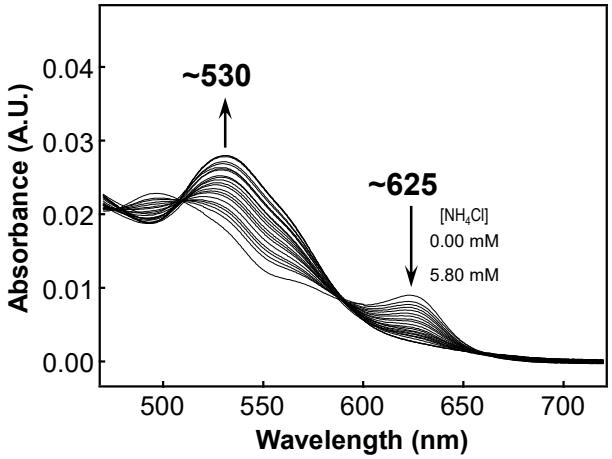

Figure S9 Absorption spectra (470–720 nm) of Peptide-Heme(Fe^{3+})-H_2O/G4 hybrid complex in the presence of various concentrations of NH_4Cl, in 300 mM KCl and 500 mM Tris-HCl buffer (pH 8.50 at 25 °C) containing 0.08 w/v% TritonX-100 and 0.5 v/v% dimethyl sulfoxide. For sample preparation of the Peptide-Heme(Fe^{3+})-H_2O/G4 hybrid-complex, 400 μL of 6 μM Peptide-Heme-H_2O was mixed with 400 μL of 30 μM $[d(TTAGGG)]_4$.

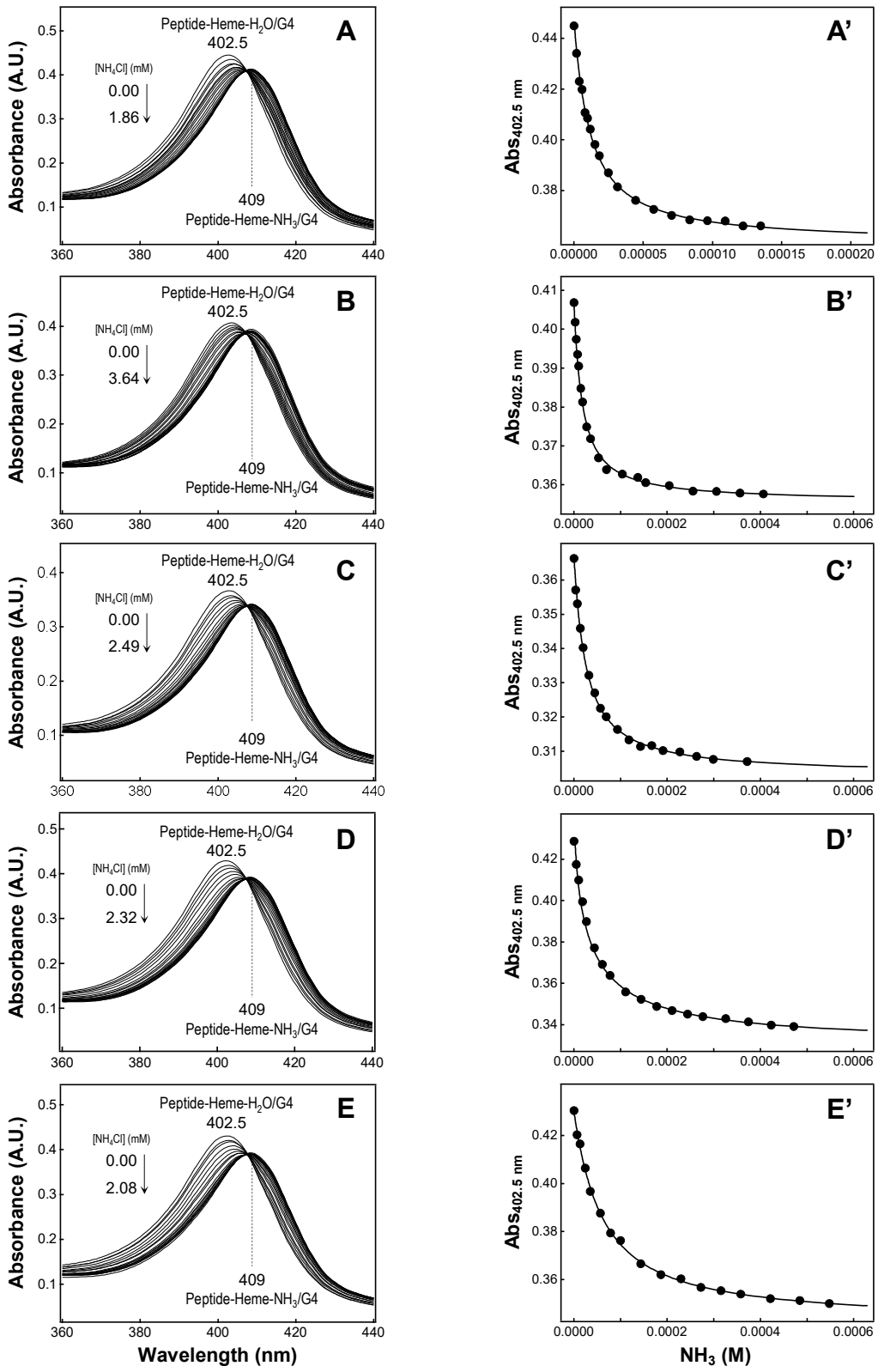

Figure S10 (A-E) Absorption spectra (360–440 nm) of Peptide-Heme(Fe^{3+})-H_2O/G4 hybrid complex in the presence of various concentrations of NH_4Cl, in 300 mM KCl and 500 mM Tris-HCl buffer (pH 8.50 at 15–35 °C) containing 0.08 w/v% TritonX-100 and 0.5 v/v% dimethyl sulfoxide. (A'-E') A plot of the 402.5 nm absorbance against NH_3 concentration. (A and A') 15 °C, [Peptide-Heme] = 3.6 μM, [G4] = 16.5 μM; (B and B') 20 °C, [Peptide-Heme] = 3.3 μM, [G4] = 13.8 μM; (C and C') 25 °C, [Peptide-Heme] = 3.0 μM, [G4] = 12.5 μM; (D and D') 30 °C, [Peptide-Heme] = 3.5 μM, [G4] = 10.5 μM; (E and E') 35 °C, [Peptide-Heme] = 3.5 μM, [G4] = 10.5 μM.

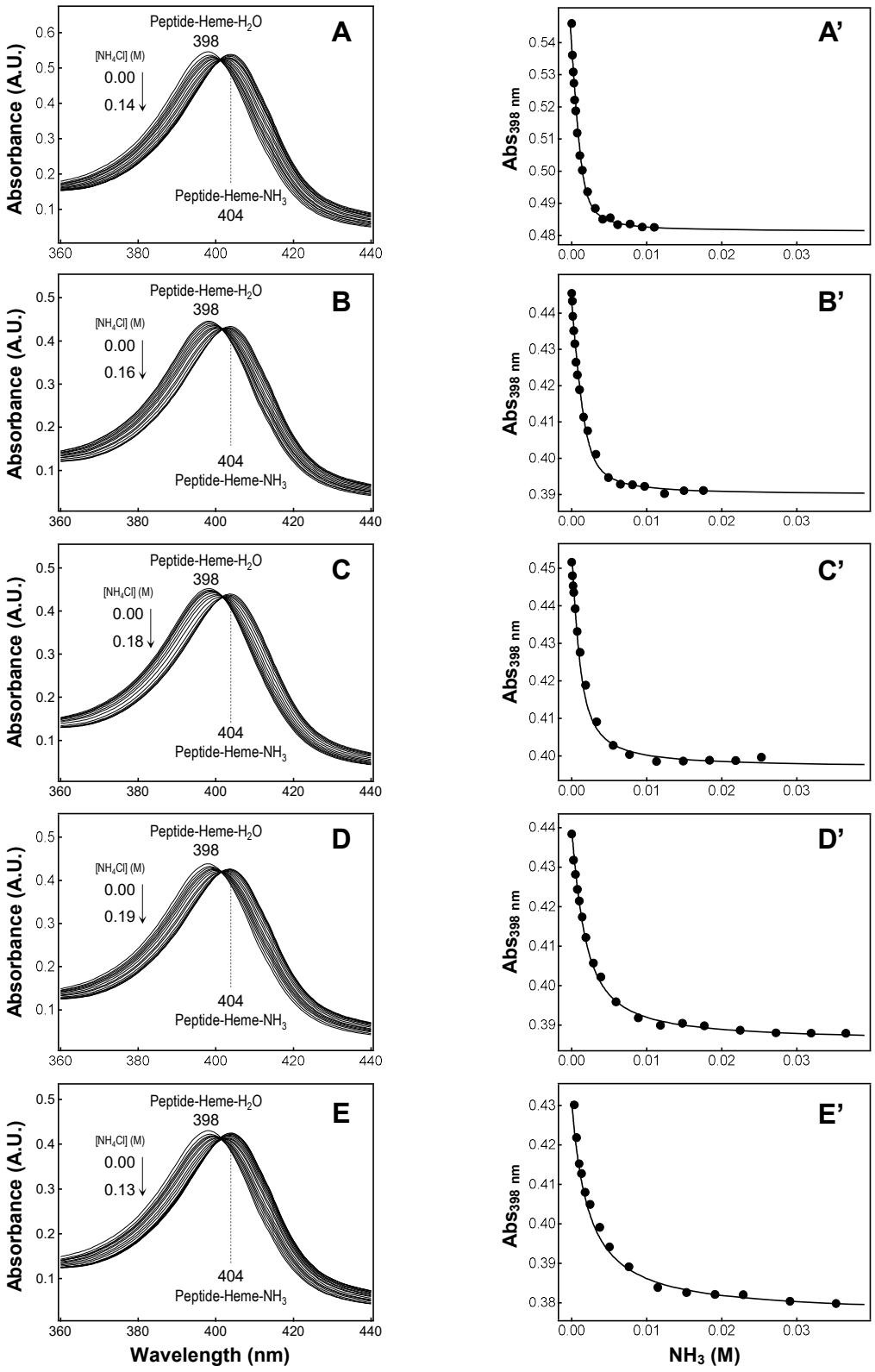

Figure S11 (A-E) Absorption spectra (360–440 nm) of Peptide-Heme(Fe^{3+})-H_2O in the presence of various concentrations of NH_4Cl, in 300 mM KCl and 500 mM Tris-HCl buffer (pH 8.50 at 15–35 °C) containing 0.08 w/v% TritonX-100 and 0.5 v/v% dimethyl sulfoxide. (A'-E') A plot of the 398 nm absorbance against NH_3 concentration. (A and A') 15 °C, [Peptide-Heme] = 4.2 μM; (B and B') 20 °C [Peptide-Heme] = 3.4 μM; (C and C') 25 °C, [Peptide-Heme] = 3.5 μM; (D and D') 30 °C, [Peptide-Heme] = 3.4 μM; (E and E') 35 °C, [Peptide-Heme] = 3.3μM.

Table S3 NH_3 binding constants (K_s) for ligand substitution reaction.

Temperature (°C)	K_s (M^{-1})	
	Peptide-Heme	Peptide-Heme/G4
15	4438 ± 164	98733 ± 7141
20	2706 ± 159	61221 ± 2011
25	1606 ± 303	41227 ± 1368
30	825 ± 41	27873 ± 2084
35	528 ± 42	18357 ± 284

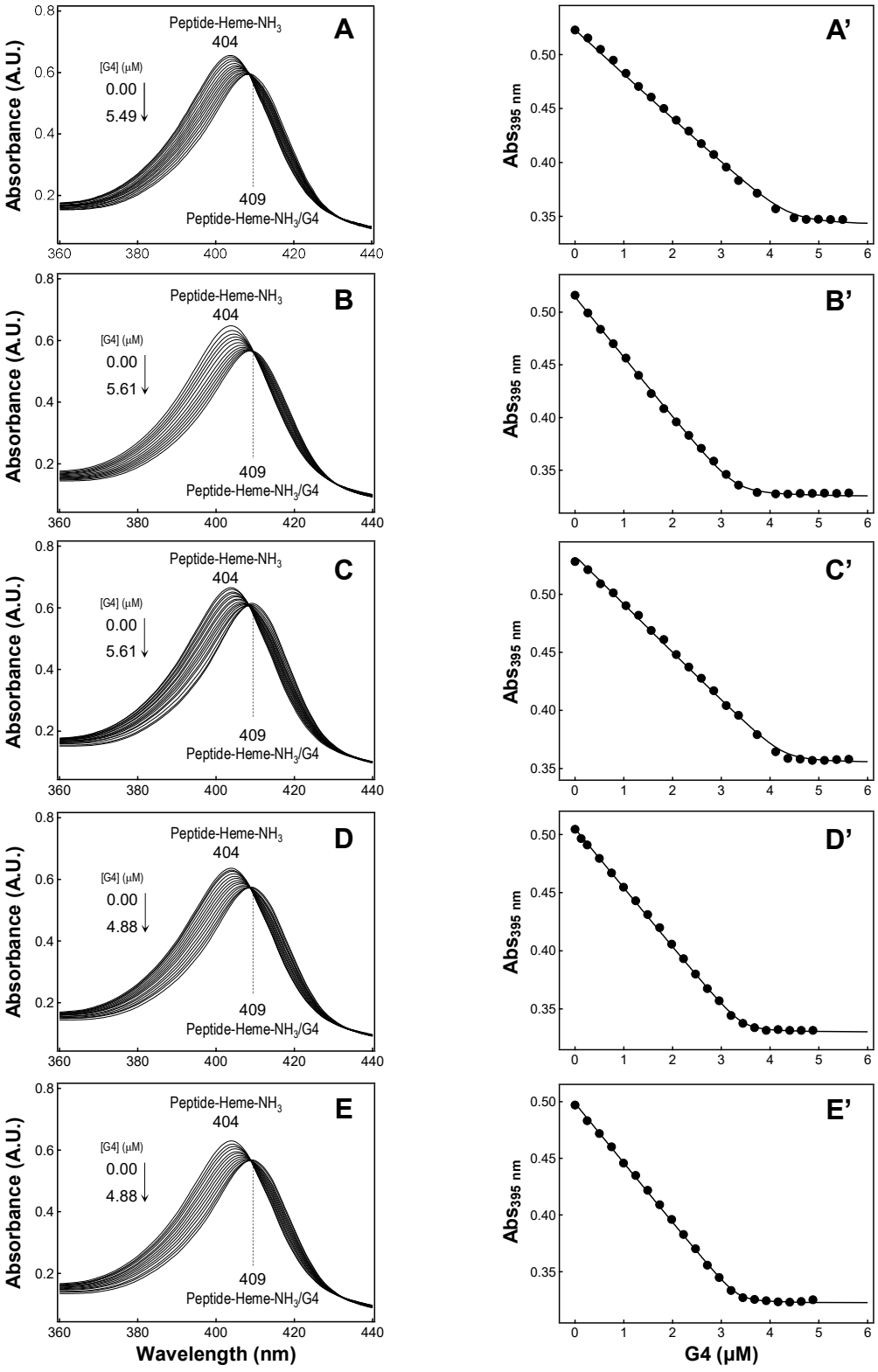

Figure S12 (A-E) Absorption spectra (360–440 nm) of Peptide-Heme(Fe^{3+})-NH_3 in the presence of various concentrations of $[d(TTAGGG)]_4$, in 100−180 mM NH_4Cl, 300 mM KCl, and 500 mM Tris-HCl buffer (pH 8.50 at 15−35 °C) containing 0.08 w/v% TritonX-100 and 0.5 v/v% dimethyl sulfoxide. (A'-E') A plot of the 395 nm absorbance against $[d(TTAGGG)]_4$ concentration. (A and A') 15 °C, [Peptide-Heme] = 5 μM, $[NH_4Cl]$ = 100 mM; (B and B') 20 °C, [Peptide-Heme] = 5 μM, $[NH_4Cl]$ = 100 mM; (C and C') 25 °C, [Peptide-Heme] = 5 μM, $[NH_4Cl]$ = 100 mM; (D and D') 30 °C, [Peptide-Heme] = 5 μM, $[NH_4Cl]$ = 150 mM; (E and E') 35 °C, [Peptide-Heme] = 5 μM, $[NH_4Cl]$ = 180 mM.

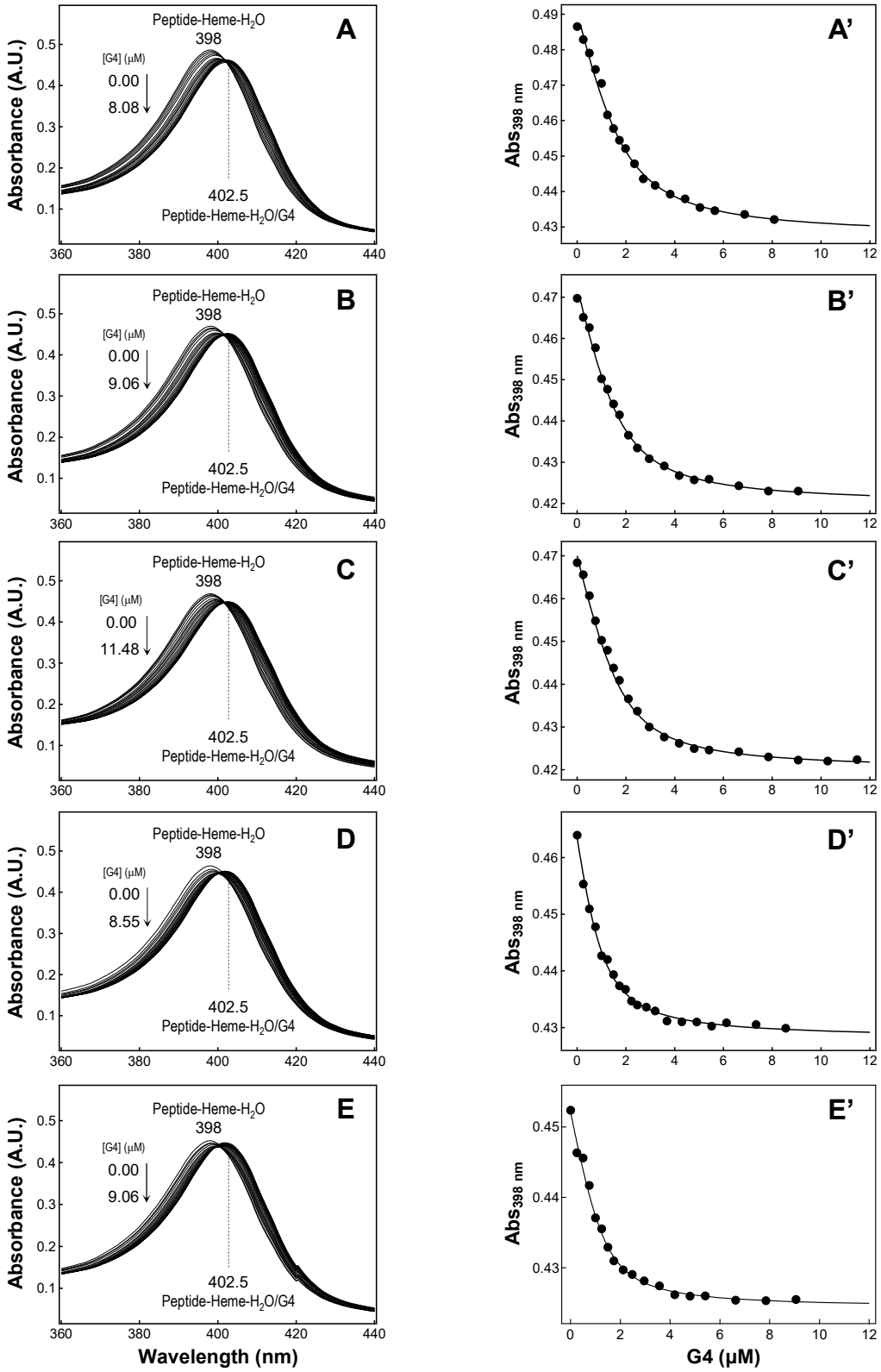

Figure S13 (A-E) Absorption spectra (360–440 nm) of Peptide-Heme(Fe^{3+})-H_2O in the presence of various concentrations of $[d(TTAGGG)]_4$, in 300 mM KCl and 500 mM Tris-HCl buffer (pH 8.50 at 15–35 °C) containing 0.08 w/v% TritonX-100 and 0.5 v/v% dimethyl sulfoxide. (A'-E') A plot of the 398 nm absorbance against $[d(TTAGGG)]_4$ concentration. (A and A') 15 °C, [Peptide-Heme] = 3.7 μM; (B and B') 20 °C, [Peptide-Heme] = 3.6 μM; (C and C') 25 °C, [Peptide-Heme] = 3.6 μM; (D and D') 30 °C, [Peptide-Heme] = 3.6 μM; (E and E') 35 °C, [Peptide-Heme] = 3.5 μM.

Table S4 The binding constant (K_a) for complexation reaction.

Temperature (°C)	K_a (μM^{-1})	
	Peptide-Heme-H_2O/G4	Peptide-Heme-NH_3/G4
15	1.76 ± 0.16	37.55 ± 4.86
20	2.20 ± 0.08	49.57 ± 6.79
25	2.50 ± 0.14	64.84 ± 5.32
30	3.15 ± 0.29	93.89 ± 6.44
35	4.04 ± 0.10	121.75 ± 3.00

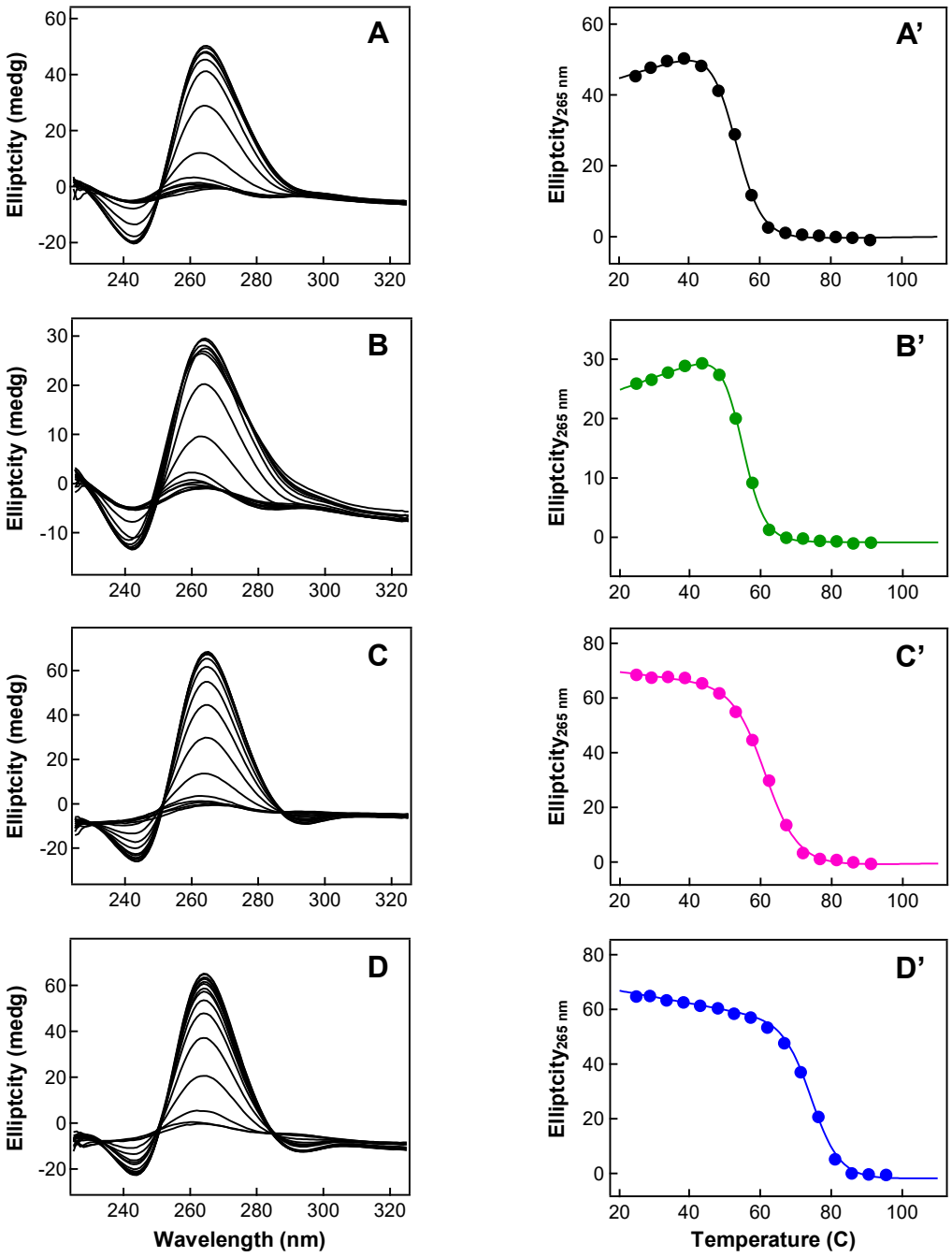

Figure S14 Temperature dependent CD spectra of $[d(TTAGGG)]_4$ (A), $[d(TTAGGG)]_4$ + NH_4Cl (B), $[d(TTAGGG)]_4$ + AcMP11 + H_2O (C), and $[d(TTAGGG)]_4$ + AcMP11 + NH_4Cl (D) in 100 mM KCl and 50 mM TAPS buffer (pH 8.50 at 25 °C). CD melting curve of $[d(TTAGGG)]_4$ (A'), $[d(TTAGGG)]_4$ + NH_4Cl (B'), $[d(TTAGGG)]_4$ + AcMP11 + H_2O (C'), and $[d(TTAGGG)]_4$ + AcMP11 + NH_4Cl (D').

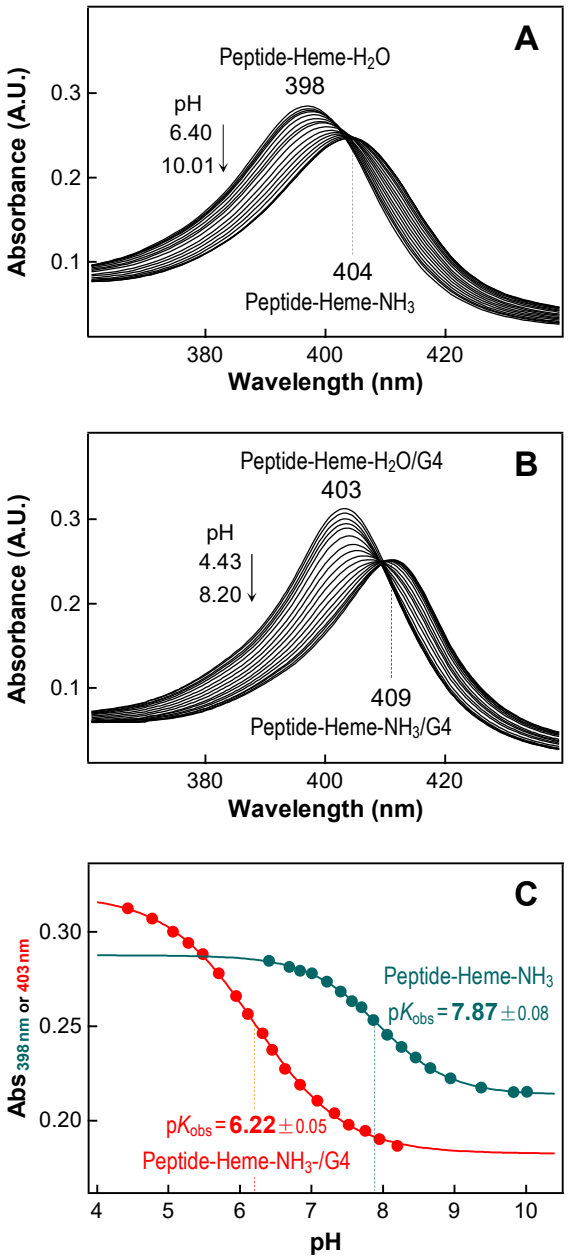

Figure S15 (A) pH-dependent absorption spectra of oxidized Peptide-Heme(Fe^{3+})/G4 hybrid complex in 20 mM NH_4Cl, 300 mM KCl, 500 mM Tris-HCl buffer at 25 °C . (B) pH-dependent absorption spectra of oxidized Peptide-Heme(Fe^{3+}) in 20 mM NH_4Cl, 300 mM KCl, 500 mM Tris-HCl buffer at 25 °C. (C) Plots of the 398 or 403 nm aborbance of the oxidized Peptide-Heme(Fe^{3+})/G4 (red) and Peptide-Heme(Fe^{3+}) (black), respectively, against pH at 25 °C. For sample preparation of the Peptide-Heme(Fe^{3+})/G4 hybrid-complex, 400 μL of 6 μM Peptide-Heme(Fe^{3+}) was mixed with 400 μL of 60 μM $[d(TTAGGG)]_4$.

Table S5 The pK_a values of NH_4^+ in aqueous solution at 15–35 °C.[a]

Temperature (°C)	15	20	25	30	35
pK	9.564	9.400	9.245	9.093	8.947

[a] Data taken from Speight JG. *Lange's Handbook of Chemistry*. 17th ed. McGraw-Hill Education, 2017.